Measurements of the Longitudinal Development of Air Showers with the Pierre Auger Observatory

DIEGO GARCIA-PINTO[1] FOR THE PIERRE AUGER COLLABORATION[2]
[1]*Universidad Complutense de Madrid, Madrid, Spain*
[2]*Observatorio Pierre Auger, Av. San Martin Norte 304, 5613 Malargüe, Argentina*
(Full author list: http://www.auger.org/archive/authors_2011_05.html)
auger_spokespersons@fnal.gov
DOI: 10.7529/ICRC2011/V02/0709

Abstract: Due to its hybrid design, the Pierre Auger Observatory provides a variety of independent experimental observables that carry information on the characteristics of the longitudinal development of ultra-high energy air showers. These include the direct measurement of the profile of the energy deposit of showers in the atmosphere through the detection of fluorescence light but also observables derived from the shower signal measured with the surface detector array. In this contribution we present a comparison of the results obtained with the fluorescence detector on the depth of shower maximum with complementary information derived from asymmetry properties of the particle signal in the surface detector stations and the depth profile of muon production points, also derived from surface detector data. The measurements are compared to predictions for proton- and iron-induced showers.

Keywords: UHECR, The Pierre Auger Observatory, mass composition, hadronic interactions

1 Introduction

The properties of ultra-high energy cosmic rays (UHECRs) can be studied by measuring the extensive air showers (EAS) that they produce in the atmosphere. For example, information on the mass of the primary particles can, in principle, be derived from the longitudinal depth profiles of these showers. However, the longitudinal development of the showers are strongly affected by the mass composition of cosmic rays and by the features of the hadronic interactions, both of which vary with energy in a manner that is unknown. If one were confident about the behaviour of one of these quantities then the behaviour of the other could be deduced.

In this article we present the measurement of four independent observables that are closely related to the longitudinal depth profile of air showers and hence, sensitive to primary mass composition. Due to the different character of the observables employed, a direct comparison of the measurement results is not possible. Instead, the data are compared to predictions from air shower simulations. Modelling uncertainties are considered by using the three different interaction models EPOS, QGSJET II, and SIBYLL [1], but it is understood that the differences between these models might not fully represent the theoretical uncertainties [2].

2 Measurements of the Longitudinal Shower Development

With the Pierre Auger Observatory [3] information on the shower development can be extracted using both the Surface Detector (SD) and the Fluorescence Detector (FD). The SD consists of more than 1660 detector stations covering an area of approximately $3000\,\mathrm{km}^2$. Each SD unit is a water-Cherenkov detector with electronics that digitises the signal at 40 MHz sampling rate. The FD has a total of 27 optical telescopes arranged in five sites overseeing the SD.

The observation of showers with the FD allows us to directly measure the most important observable to characterise the longitudinal profile of a shower, the depth of the shower maximum, $X_{\max}$, i.e. the depth at which air showers deposit the maximum energy per unit mass of atmosphere traversed [4]. On the other hand, the SD provides observables which are related to the longitudinal shower profile as well. These observables are subject to independent systematic uncertainties (both experimentally and theoretically). Moreover the higher statistics of showers measured with the SD allows us to reach higher energies than with the FD.

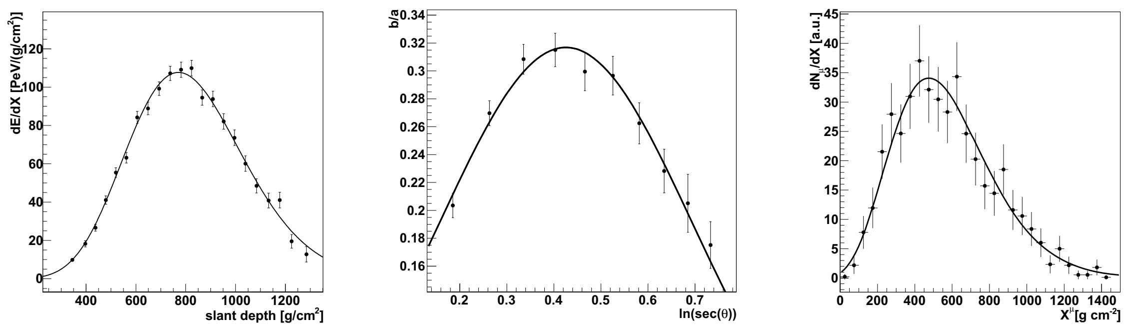

Figure 1: Typical longitudinal development of the energy deposit (left panel), of the average asymmetry in the risetime (centre panel) and the muon production depth (right panel).

2.1 Depth of Shower Maximum

The measurement of the longitudinal profile of the energy deposit in the atmosphere with the Pierre Auger Observatory is described in [4]. In this analysis hybrid events, i.e. showers observed simultaneously by the FD and at least by one SD station, have been used. The longitudinal profile of the energy deposit is reconstructed by the FD from the recorded fluorescence and Cherenkov light signals. The collected light is corrected for the attenuation between the shower and the detector using data from atmospheric monitoring devices. The longitudinal shower profile is reconstructed as a function of the atmospheric depth and $X_{\rm max}$ is obtained by fitting the profile with a Gaisser-Hillas function. A typical longitudinal profile of the energy deposit of one shower is shown in the left panel of Fig. 1.

The $X_{\rm max}$ results presented here are an update of [4]. Hybrid events recorded between December 2004 and September 2010 with reconstructed energy above 10^{18} eV have been used for the present analysis. To obtain a good resolution in the measurement of $X_{\rm max}$, several quality cuts are applied. The cuts and their effects are described fully in [5]. After all cuts, 6744 events are selected for the $X_{\rm max}$ analysis. The average values of the shower maximum, $\langle X_{\rm max}\rangle$, as a function of energy are displayed in Fig. 2, alongside predictions from several models. Uncertainties of the atmospheric conditions, calibration, event selection and reconstruction give rise to a systematic uncertainty of $\leq 13\ {\rm g/cm^2}$ [4] which corresponds to $\lesssim 13\ \%$ of the proton-iron separation predicted by the models. Since the $X_{\rm max}$ resolution of the FD is at the level of 20 ${\rm g/cm^2}$ above a few EeV, the intrinsic shower-to-shower fluctuations, RMS($X_{\rm max}$), can be measured as well, see lower panel of Fig. 2.

2.2 Asymmetry of Signal Risetime

For each SD event, the water-Cherenkov detectors record the signal as a function of time. The first part of the signal is dominated by the muon component which arrives earlier and over a period of time shorter than the electromagnetic particles, since muons travel in almost straight lines whereas the electromagnetic particles suffer more multiple scattering on their way to ground. Due to the absorption of the electromagnetic (EM) component, the number of these particles at the ground depends, for a given energy, on the distance to the shower maximum and therefore on the primary mass. In consequence, the time profile of particles reaching ground is sensitive to cascade development as the higher is the production height the narrower is the time pulse.

The time distribution of the SD signal is characterised by means of the risetime (the time to go from 10% to 50% of the total integrated signal), $t_{1/2}$, which depends on the distance to the shower maximum, the zenith angle θ and the distance to the core r. In previous studies [6] the risetime was related to the shower maximum using a subset of hybrid events. Using this correlation it is possible to measure the shower evolution with surface detector data.

The azimuthal asymmetry of $t_{1/2}$ from water-Cherenkov detector signals of non-vertical showers carries information about the longitudinal development of the showers [7]. Unfortunately it is not possible to define the asymmetry on an event-by-event basis, therefore the risetime asymmetry is obtained by grouping events in bins of energy and $\sec\theta$. A key parameter for the analysis is the angle ζ, the azimuth angle in the shower plane (the plane perpendicular to the shower axis). Detectors that are struck early in the development of the shower across the array have values of this angle in the range $-\pi/2 < \zeta < \pi/2$ with $\zeta = 0°$ corresponding to the vertical projection of the incoming direction onto the shower plane. For each (E, $\sec\theta$) bin a fit of $\langle t_{1/2}/r\rangle = a + b\cos\zeta$ provides the asymmetry amplitude, b/a. For a given energy, the b/a value changes with the zenith angle, i.e. distance to the shower maximum. The evolution of b/a with zenith angle is thus reminiscent of the longitudinal development of the shower and has a maximum which is different for different primaries [8]. For each energy bin, the asymmetry amplitude is fitted using a Gaussian function of $\ln(\sec\theta)$. This allows the determination of the position of the maximum, $\Theta_{\rm max}$, defined as the value of $\sec\theta$ for which b/a is maximum. In Fig.1, centre

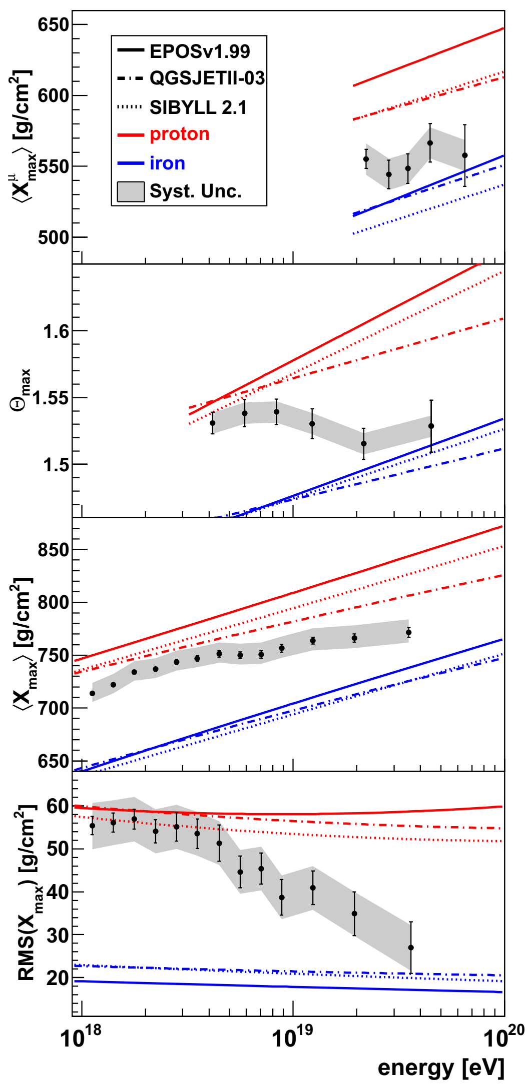

Figure 2: Results on shower evolution sensitive observables compared with models prediction. The error bars correspond to the statistical uncertainty. The systematic uncertainty is represented by the shaded bands.

panel, an example of b/a as a function of $\ln(\sec\theta)$ and the corresponding fit to obtain $\Theta_{\rm max}$ is shown for the energy bin of $\log(E/\mathrm{eV}) = 18.85 - 19.00$.

Data collected with the surface detector of the Pierre Auger Observatory from January 2004 to December 2010 have been used for the $\Theta_{\rm max}$ analysis, with a total of 18581 events surviving the following cuts. Events are required to satisfy the trigger levels described in [9] and to be in the regime of full array efficiency for all primary species: $E > 3.16 \times 10^{18}$ eV and $\theta \leq 60°$. For selected events, detectors are used in the analysis if the signal size is above 10 VEM and not saturated and if they have core distances between 500 m and 2000 m. The measured values of $\Theta_{\rm max}$ obtained for 6 bins of energy above 3.16×10^{18} eV are shown in Fig. 2. The systematic uncertainty in the measured values of $\Theta_{\rm max}$ has been evaluated taking into account its possible sources: reconstruction of the core of the shower, event selection and risetime vs core distance parameterisation and amounts to $\lesssim 10\%$ of the proton-iron separation predicted by the models. We note that muon numbers predicted by EAS simulations differ from those observed in data [2]. A preliminary study, using a normalisation of 1.6 [2], indicates a possible change of about $\leq 5\%$ of the proton-iron difference.

As mentioned above, the shower observables $\Theta_{\rm max}$ and $X_{\rm max}$ are expected to be correlated as both are dependent upon the rate of shower development. The correlation between $\Theta_{\rm max}$ and $X_{\rm max}$ shown in Fig. 3 has been obtained with hybrid data using criteria similar to those adopted in [4]. In Fig. 3 the $\Theta_{\rm max}$ vs $X_{\rm max}$ correlations found with Monte Carlo data are also shown for proton and iron primaries, demonstrating that the correlation is independent of the primary mass.

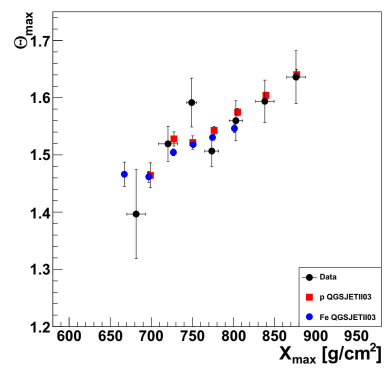

Figure 3: $\Theta_{\rm max}$ vs $X_{\rm max}$. Black dots correspond to data, while Monte Carlo results for proton(iron) primary are indicated by red(blue) squares(circles).

2.3 Depth Profile of Muon Production Points

Using the time information of the signals recorded by the SD it is also possible to obtain information about the longitudinal development of the hadronic component of extensive air showers in an indirect way. In [10] a method is presented to reconstruct the Muon Production Depth (MPD), i.e. the depth at which a given muon is produced measured parallel to the shower axis, using the FADC traces of detectors far from the core. The MPD technique allows us to convert the time distribution of the signal recorded by the SD detectors into muon production distances using an approximate relation between production distance, transverse distance and time delay with respect the shower front plane. From the MPDs an observable can be defined, $X^{\mu}_{\rm max}$, as the depth along the shower axis where the number of produced muons reaches a maximum. This new observable is a parameter sensitive to the longitudinal shower evolution which, as in the case of $\Theta_{\rm max}$, can be obtained with the information provided by the SD alone (see [11] for detailed explanation of the analysis). The method is currently restricted to inclined showers where muons dominate the signal at ground level (studies to extend the analysis to vertical showers are ongoing). Once the MPD is obtained for each event, the value of $X^{\mu}_{\rm max}$ is found by fitting a Gaisser-Hillas function to the depth profile. An example of the MPD profile and the result of the Gaisser-Hillas fit of a particular event with $E \approx 95$ EeV and zenith angle $\theta \approx 60^{\circ}$ is shown in the right panel of Fig. 1.

The results of $\langle X^{\mu}_{\rm max}\rangle$ presented here are based on data collected between January 2004 and December 2010, with zenith angles between 55° and 65°. The angular window was chosen as a trade-off between muon to EM ratio and the reconstruction uncertainty. The finite time resolution in the FADC traces produces an uncertainty on the reconstruction that decreases with the core distance and increases with the zenith angle. Thus, to keep these distortions low, only detectors far from the core (r $>$ 1800 m) can be used. This distance restriction imposes a severe limitation in the energy range where the method can by applied. Therefore only events with reconstructed energy larger than 20 EeV are used. After applying a set of reconstruction and quality cuts (see [11] for a complete description of the cuts), a total of 244 events are selected. The measured values of $\langle X^{\mu}_{\rm max}\rangle$ are presented in the upper panel of Fig. 2. The systematic uncertainty due to reconstruction bias, core position, rejection of the EM component and quality cuts amounts to $11\ {\rm g/cm^2}$, corresponding to about 14% of the proton-iron separation predicted by the models [11]. The predictions of $X^{\mu}_{\rm max}$ from different hadronic models (such as those shown in Fig. 2) would not be affected if a discrepancy between a model and data [2] is limited to the total number of muons. However, differences in the muon energy and spatial distribution would modify the predictions.

As for $\Theta_{\rm max}$, it is expected that the values of $X^{\mu}_{\rm max}$ will be correlated with $X_{\rm max}$. However there are insufficient events to make an experimental test such as that shown in Fig. 3. In Fig. 4 the results of model calculations are displayed using QGSJETII-03 as the hadronic model: the anticipated correlation is seen.

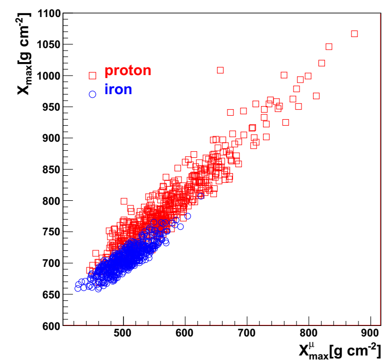

Figure 4: $X_{\rm max}$ vs $X^{\mu}_{\rm max}$ obtained for proton and iron simulated showers using QGSJETII-03 hadronic interaction model.

3 Conclusions

It is clear from Fig. 2 that if the models give a fair representation of the theoretical systematics of air shower modelling, then one might infer the primary composition from the data on the longitudinal air shower development presented here.

The evolution of $\langle X_{\rm max}\rangle$, $\Theta_{\rm max}$ and $\langle X^{\mu}_{\rm max}\rangle$ with energy is similar, despite the fact that the three analyses come from completely independent techniques that have different sources of systematic uncertainties. Concerning the RMS of $X_{\rm max}$, a variety of compositions can give rise to large values of the RMS, because the width of the $X_{\rm max}$ is influenced by both, the shower-to-shower fluctuations of individual components and their relative displacement in terms of $\langle X_{\rm max}\rangle$. However, within experimental uncertainties, the behaviour of $\langle X_{\rm max}\rangle$, $\Theta_{\rm max}$ and $\langle X^{\mu}_{\rm max}\rangle$ as shown in Fig. 2 is compatible with the energy evolution of RMS($X_{\rm max}$). In particular, at the highest energies all four analyses show consistently that our data resemble more the simulations of heavier primaries than pure protons.

References

[1] N. N. Kalmykov, S. S. Ostapchenko, and A. I. Pavlov, (1997) Nucl. Phys. Proc. Suppl. **52B**: 17-28; E.-J. Ahn *et al.*, (2009), Phys. Rev. **D80**: 094003; T. Pierog and K. Werner, (2008), Phys. Rev. Lett. **101**: 171101.

[2] J. Allen for the Pierre Auger Collaboration, paper 0703, these proceedings.

[3] The Pierre Auger Collaboration, (2004), Nucl. Instrum. Meth. **A523**: 50-95.

[4] The Pierre Auger Collaboration, (2010), Phys. Rev. Lett. **104**: 091101.

[5] P. Facal for the Pierre Auger Collaboration, paper 0725, these proceedings.

[6] H. Wahlberg for the Pierre Auger Collaboration, (2009), Proc. 31st ICRC, Łódź, Poland. arXiv:0906.2319v1[astro-ph].

[7] M.T. Dova for the Pierre Auger Collaboration, (2003), Proc. 28th ICRC, Tsukuba, Japan. 369-372.

[8] M.T. Dova *et al.*, (2009), Astropart. Phys. **31**: 312-319.

[9] The Pierre Auger Collaboration, (2010), Nucl. Instrum. Meth. **A613**: 29-39.

[10] L. Cazon, R.A. Vazquez and E. Zas, (2005), Astropart. Phys. **23**: 393-409.

[11] D. Garcia-Gamez for the Pierre Auger Collaboration, paper 0735, these proceedings.

[12] D. Heck *et al.*, (1998) Report **FZKA 6019** FZ Karlsruhe; S.J. Sciutto, (1999), arXiv:astro-ph/9911331.